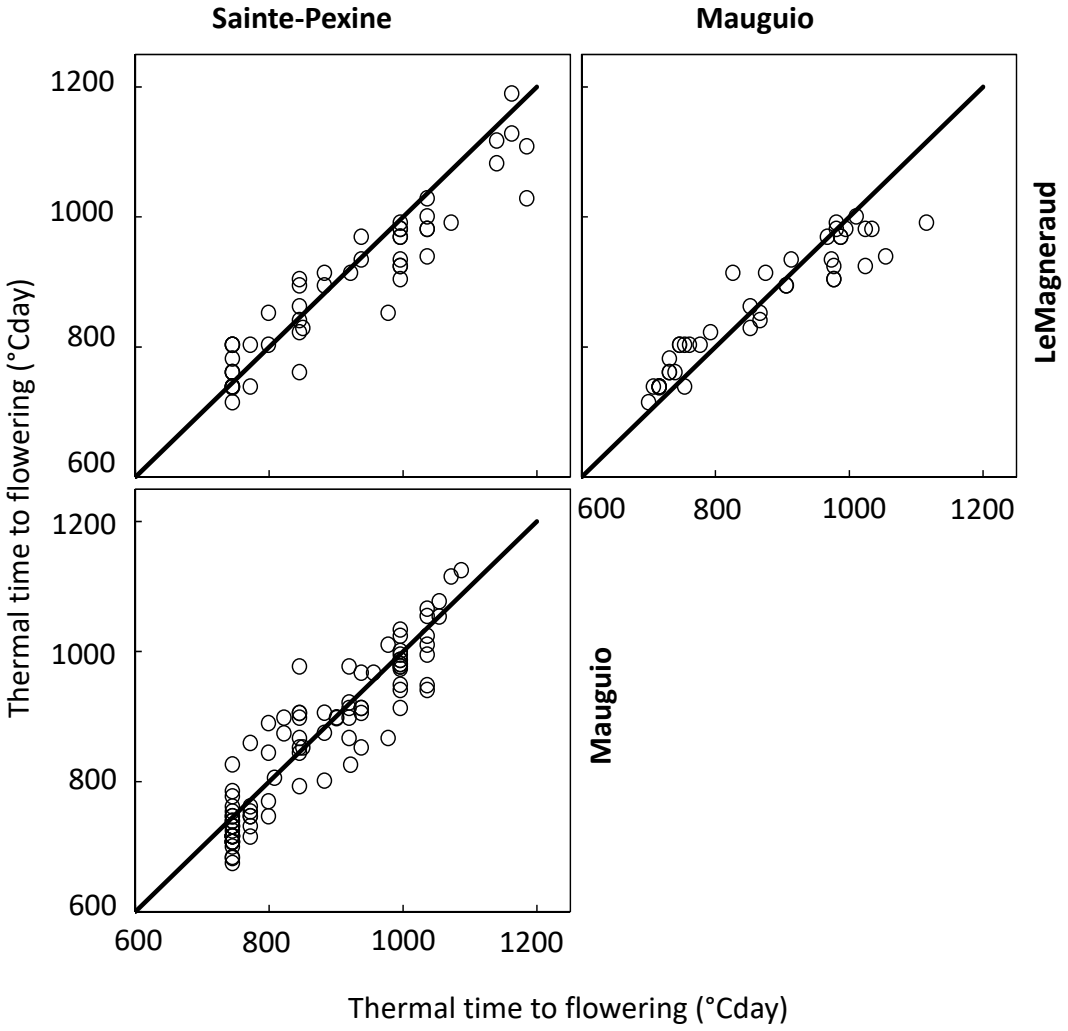

Supplementary Figure 1. Correlation between measured values of flowering time in three field experiments with full irrigation. Dots are experimental values for 121 maize accessions (57 in Le Magneraud) measured in three field experiments (LeMagneraud, France; Mauguio, France; Sainte Pexine, France). Flowering time is expressed as thermal time from sowing to anthesis. Lines are the 1:1.

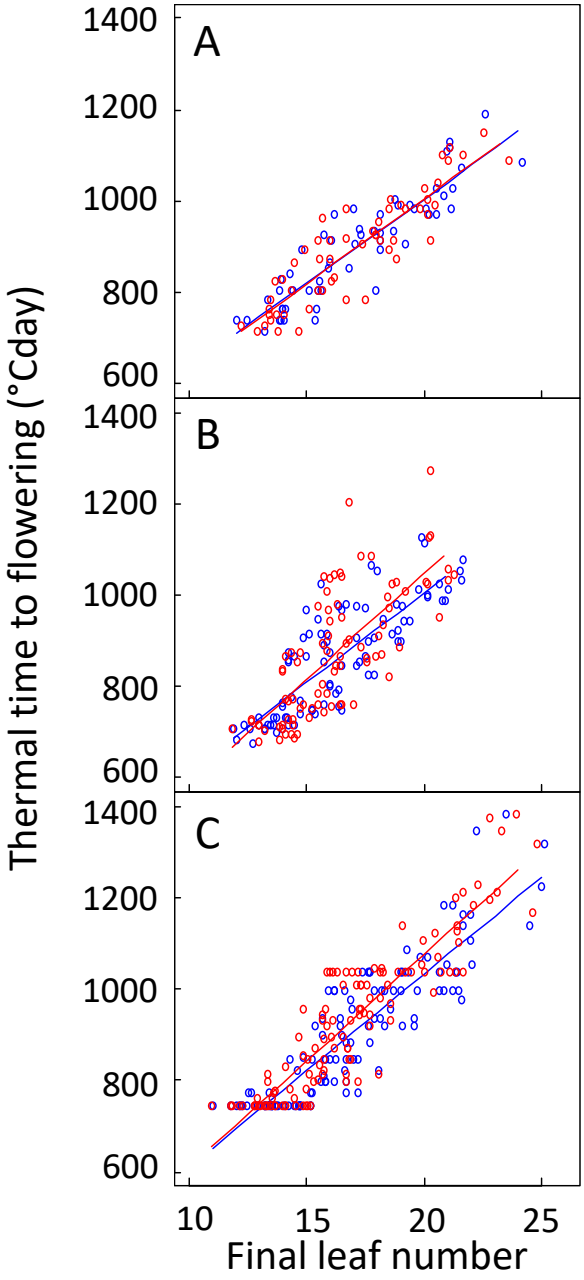

Supplementary Figure 2. Relationship between final leaf number and thermal time to flowering in three field experiments. A-C, Thermal time between sowing and flowering plotted against final leaf number for 121 maize accessions (57 in Le Magneraud) in three field experiments in irrigated (blue dots) or rainfed conditions (red dots). Dots are experimental values averaged for each accession, with ten plants per accession. **A**, LeMagneraud, France. **B**, Mauguio, France. **C,** Sainte Pexine, France.

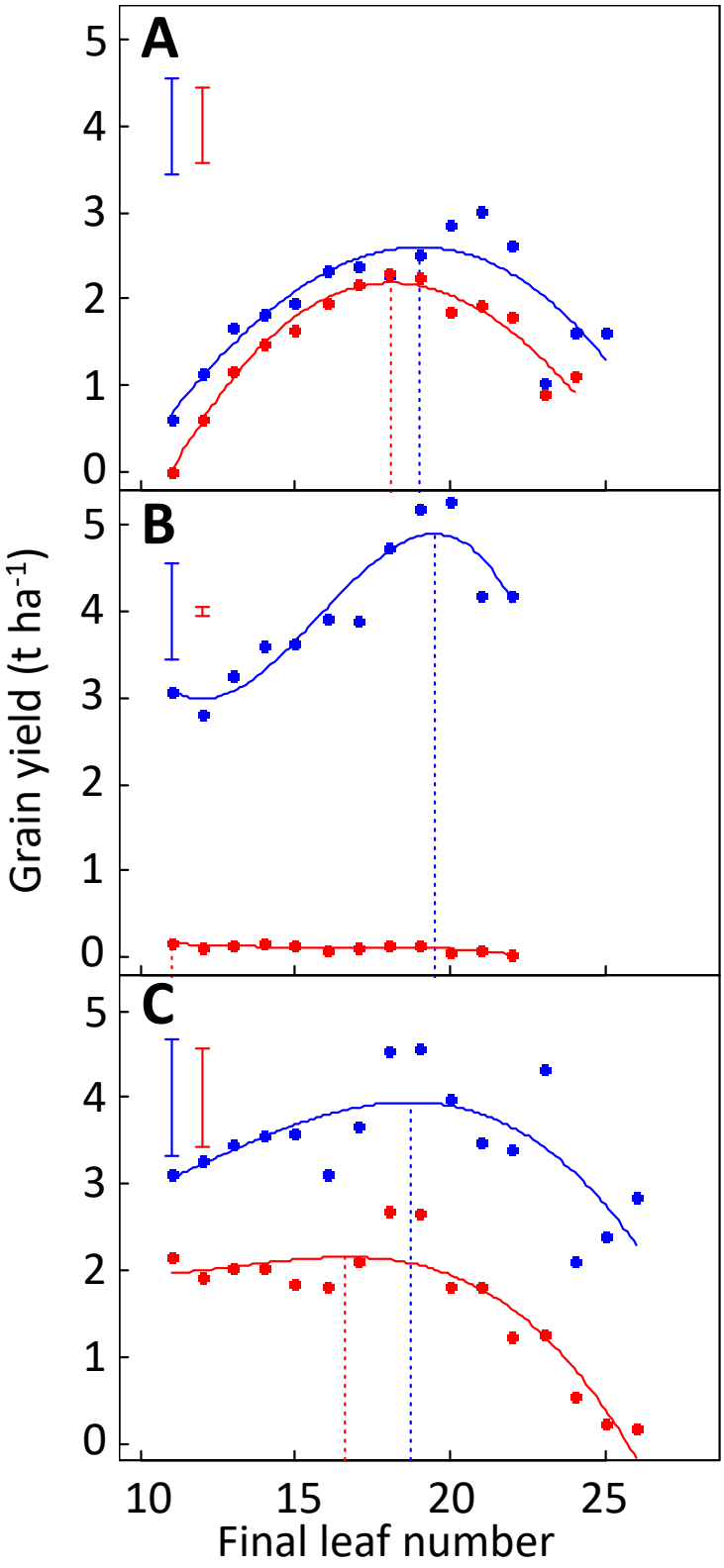

Supplementary Figure 3. Observed optimum durations of the vegetative period (sowing-flowering time), expressed in plant final leaf number in three sites and two watering regimes. Relationship between plant leaf number and yield in irrigated (blue dots and lines) or rainfed conditions (red) in three experiments with 121 maize accessions (**A**, Le Magneraud, France, 57 accessions; **B**, Mauguio, France; **C**, Sainte Pexine, France). For better intuition, the duration of the vegetative period is expressed as plant leaf number, closely related to it. Dots are mean values for maize accessions presenting a common final plant leaf number. Optimum values maximizing yield can be identified in all situations except in Mauguio in rainfed conditions, where yield was low for all accessions. Error bars, confidence intervals (P = 0.95). Plain lines, third order polynomial regressions. Vertical dashed lines, optimum cycle durations.

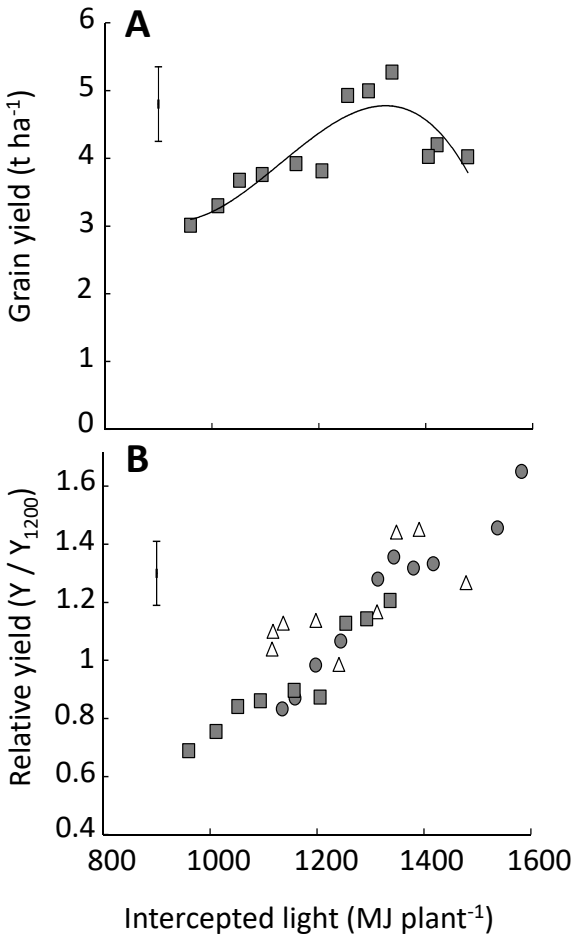

Supplementary Figure 4. Relationship between yield and intercepted light in three experiments.

A, Relationship between yield and the amount of light intercepted from emergence to 10 days after flowering for maize accessions with common plant leaf number in the irrigated treatment in Mauguio, France, 2007. The Line is a 3rd order polynomial regression.

B, Relationship between yield and intercepted light in the irrigated treatment of the three experiments (squares: Mauguio, France, 2007; circles: LeMagneraud, France, 2007; triangles: Sainte Pexine, France, 2006). Only values for varieties with final leaf number below the optimum identified in Fig. S3 are presented. For an easier comparison between experiments, yield was normalized by its value at 1200 MJ plant^{-1} predicted by the polynomial regression in each field experiment.

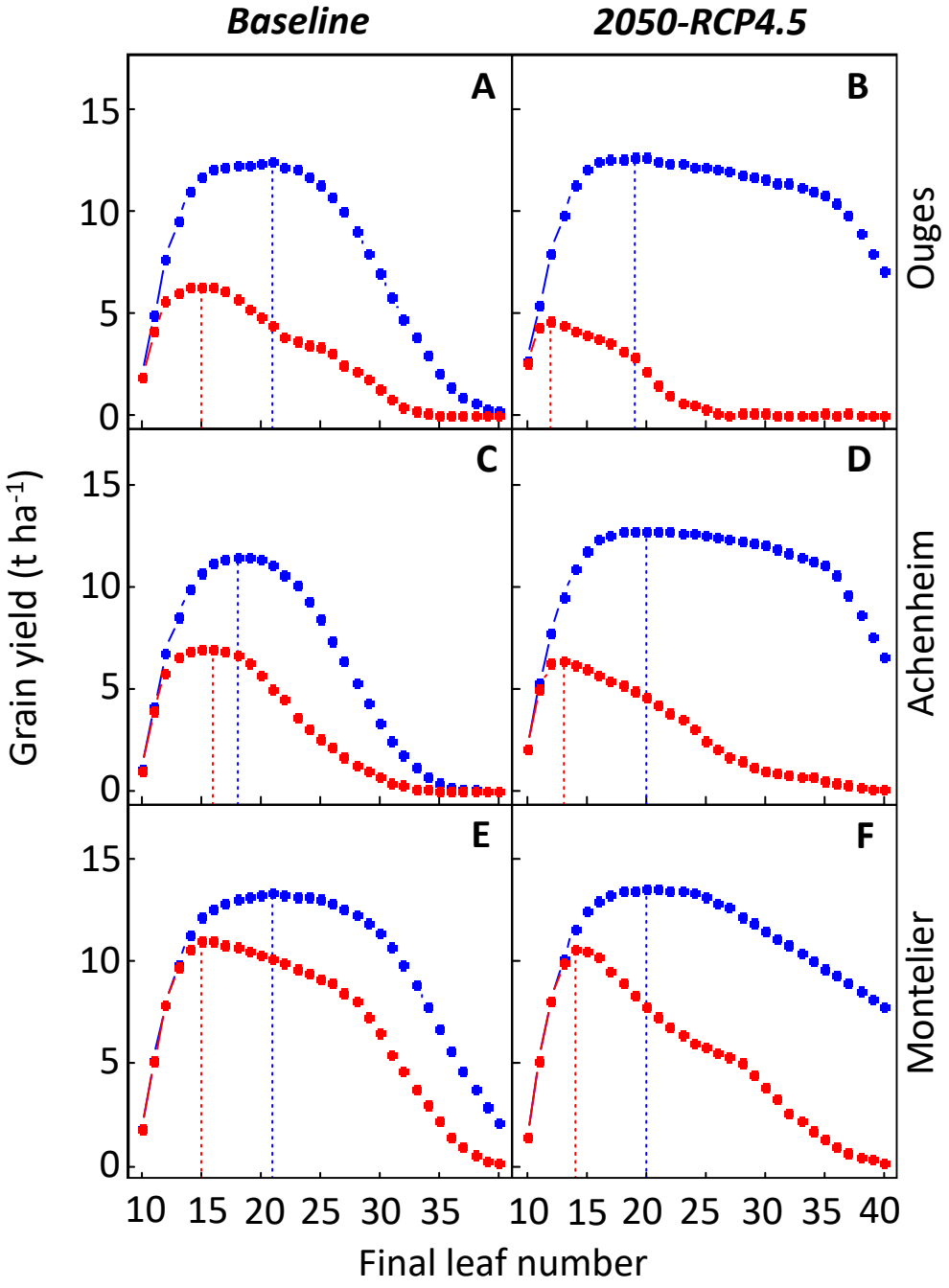

Supplementary Figure 5. Grain yield simulated for virtual varieties differing in cycle duration in three sites in current and future conditions (2050, RCP4.5). Relationship between cycle duration and yield simulated for the sites at "Ouges" (**A**,**B**), "Achenheim" (**C**,**D**) and "Montelier" (**E**,**F**) (see Table S1) in irrigated (blue dots and lines) or rainfed conditions (red dots and lines). For better intuition, cycle duration is expressed as final leaf number. Dots are averaged values for 36 years for the baseline period and 30 years and 6 GCMs for 2050. Vertical dashed lines indicate the optimum cycle duration.

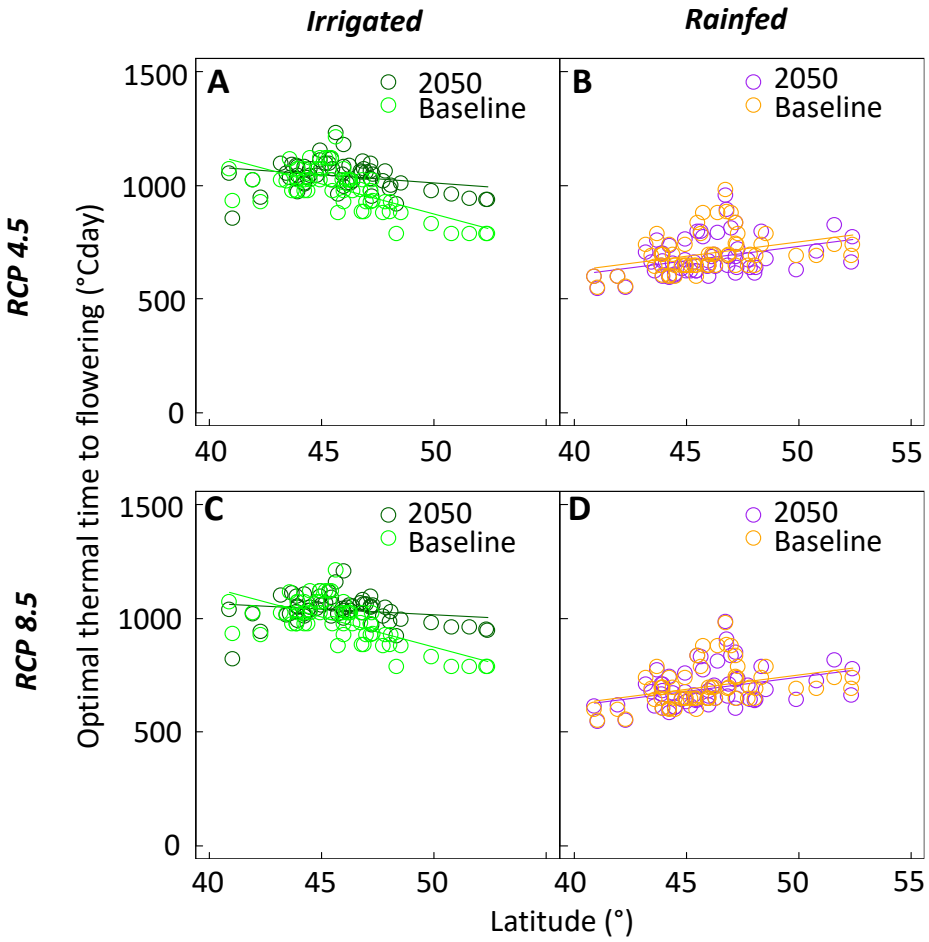

Supplementary Figure 6. Crop growth cycle duration that optimizes yield in current and future climates, as a function of latitude. A, B, C, D, Optimum time to flowering (°Cdays) as a function of latitude for the baseline period (1975-2010) and 2050 with RCP4.5 (mean of 6 GCMs) (**A**, **B**) and RCP8.5 (**C**, **D**), irrigated (**A**, **C**) or rainfed (**B**, **D**).

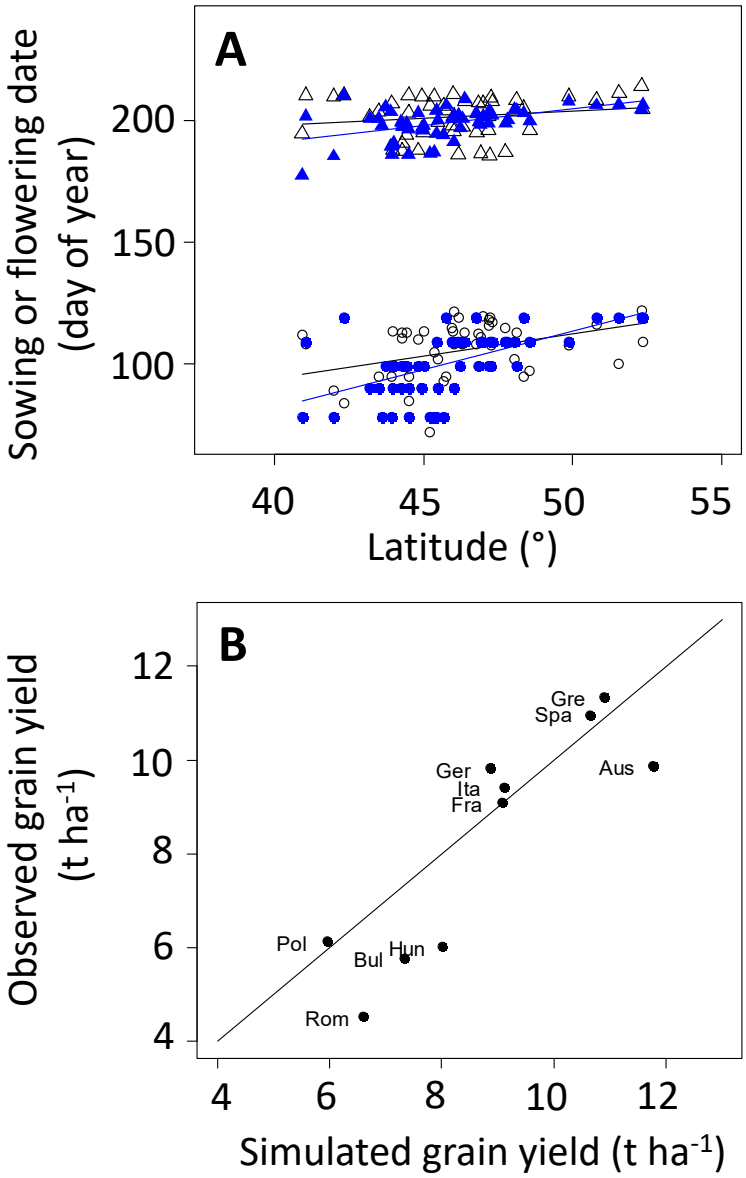

Supplementary Figure 7. Relationship between simulated and observed data .
A, Relationship between latitude and sowing or flowering dates, either simulated (blue dots) or observed (black dots, data from *AgroPhenoDB* of the Joint Research Centre). Each dot is the mean of 11 years (2000-2010) in one location, either for observed or simulated data in fully-irrigated conditions. Circles, sowing date; triangles, flowering date. Lines, linear regressions.
B, Observed and simulated yield in ten European countries. Observed values are mean values for the 2000-2010 period at country level (Eurostat database). Simulated values for the 2000-2010 period were scaled up by applying the ratio of irrigated/rainfed fields in the 25*25 km grid cell of the Eurostat database corresponding to each site(Supplementary Table 1).

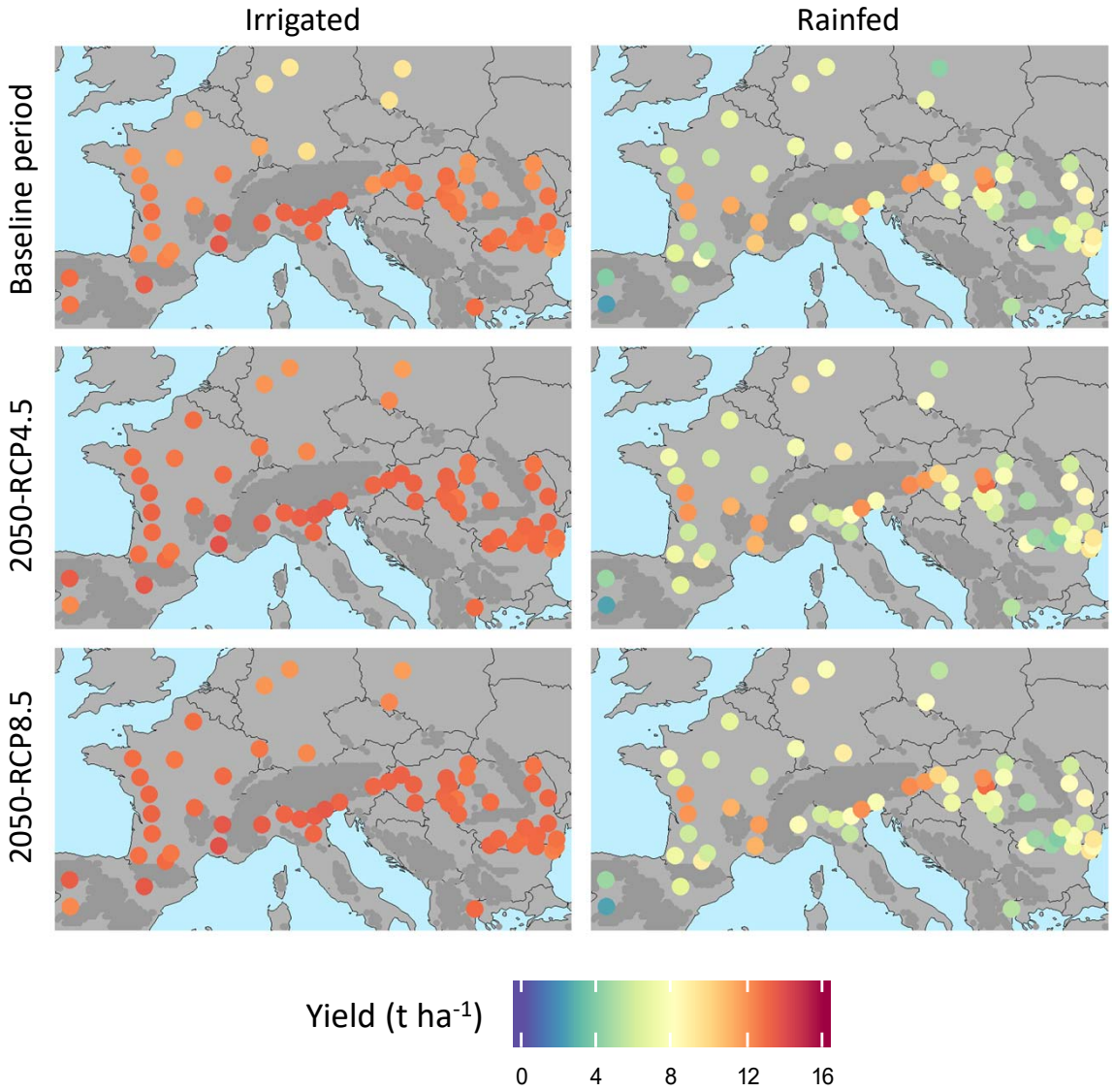

Supplementary Figure 8. Maps of simulated yield for the baseline period (1975-2010) and in 2050 (RCP4.5 and RCP8.5) in irrigated and rainfed fields. Data are averaged for 35 years for the baseline period and for 30 years and 6 GCMs for 2050 in the 59 sites. Calculations were run under the hypothesis of an increase in transpiration efficiency with CO_2 concentration.

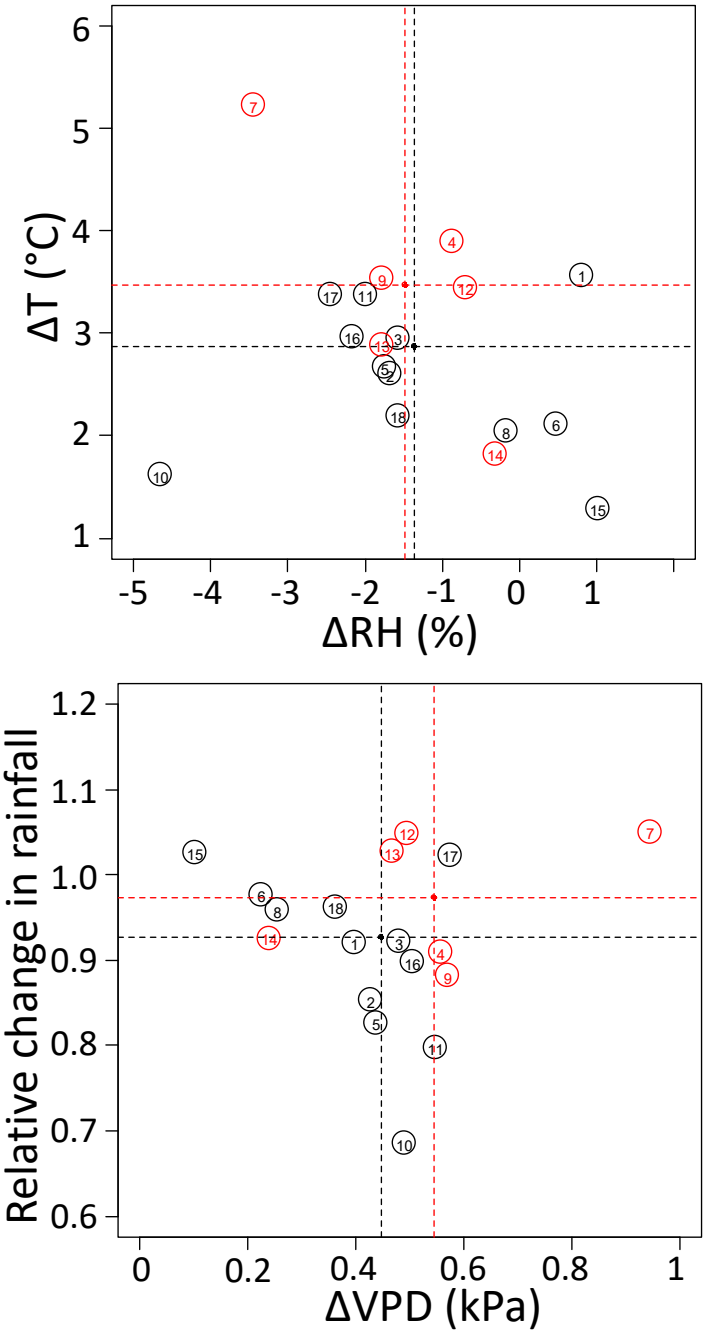

Supplementary Figure 9. Absolute changes in temperature (T), relative humidity (RH), VPD and relative changes in rainfall in June, July, and August in 2050 (RCP8.5) compared to the baseline period averaged for the 59 sites used in this study and predicted by 18 GCMs.

Each number is the average of 59 sites for one GCM. Red numbers are the six GCMs used in this study. Dotted black lines are the average for the 18 GCM. Dotted red lines are the average for the 6 GCMs used in this study. Because raw data from GCM do not include VPD and RH data, they were calculated from maximum and minimum temperatures (Tmin) of 30 simulated years, and considering that dew point temperature equals Tmin.

The 18 GCM are respectively :

(1) ACCESS1-3, (2) BCC-CSM1-1, (3) CanESM2 , (4) CMCC-CM , (5) CSIRO-MK36 , (6) EC-EARTH , (7) GFDL-CM3 , (8) GISS-E2-R-CC , (9) HadGEM2-ES , (10) INMCM4 , (11) IPSL-CM5A-MR , (12) MIROC-ESM , (13) MIROC5 , (14) MPI-ESM-MR , (15) MRI-CGCM3 , (16) NCAR-CCSM4, (17) NCAR-CESM1-CAM5 , (18) NorESM1-M.

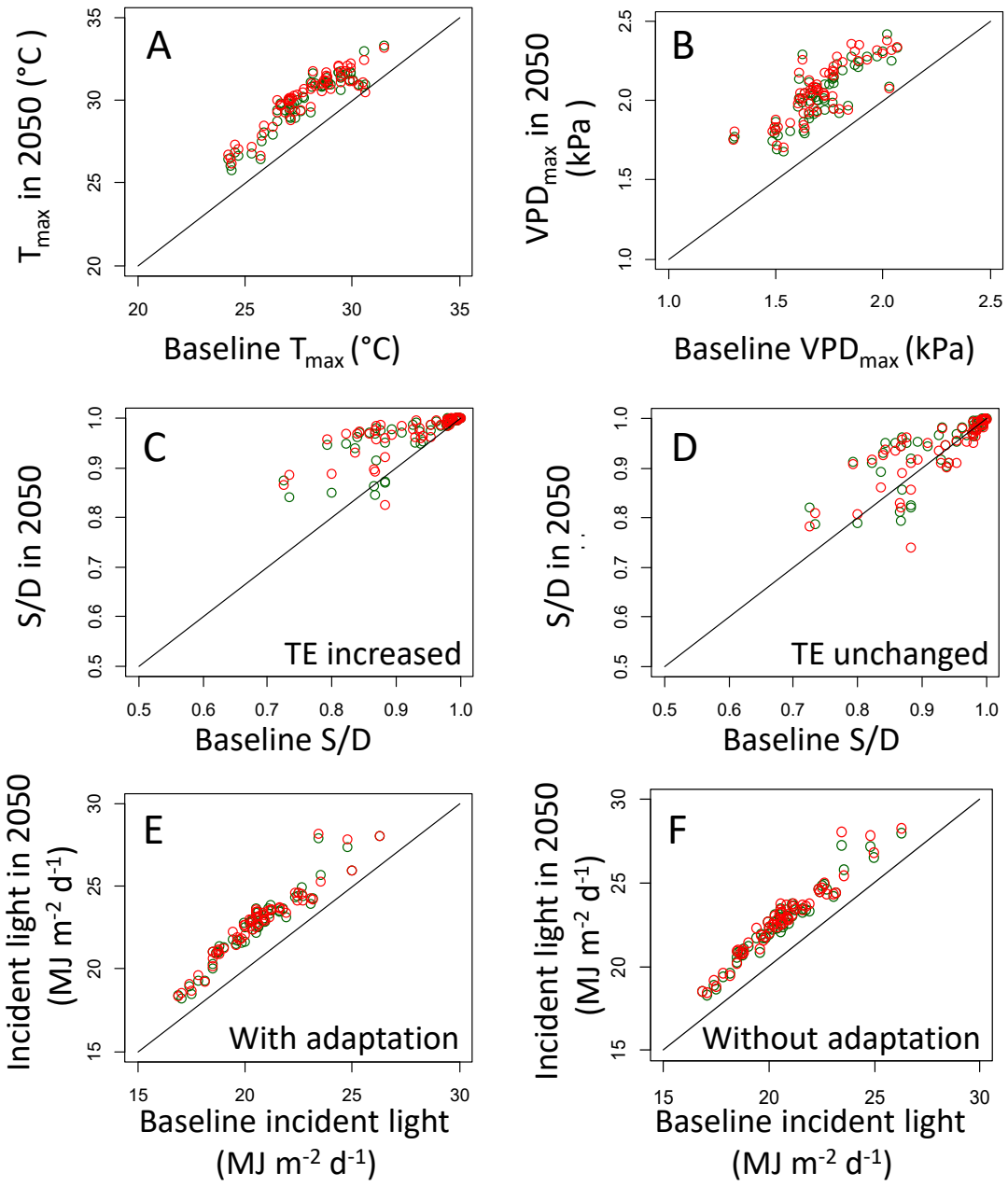

Supplementary Figure 10. Change in temperature, ratio of supply/demand for water and incident light between current and future conditions at maize flowing time. A, Mean daily maximum temperature (T_{max}) for the baseline period (1975-2010) and two RCPs in 2050. **B,** Mean daily maximum vapor pressure deficit (VPD_{max}) for the baseline period and two RCPs in 2050. **C,** Supply/demand (S/D) ratio for water for the baseline period and two RCPs in 2050, simulations carried out by considering an increase in transpiration efficiency (TE) with CO_2 concentration. **D,** S/D ratio for water for the baseline period and two RCPs in 2050 under the hypothesis of an unchanged TE. **E,** incident light for the baseline period and two RCPs in 2050 considering adaptation. **F,** incident light for the baseline period and two RCPs in 2050 considering no adaptation. Green, RCP 4.5, mean value of six GCMs for the period from anthesis to beginning of grain filling. Red, RCP8.5, same GCMs.

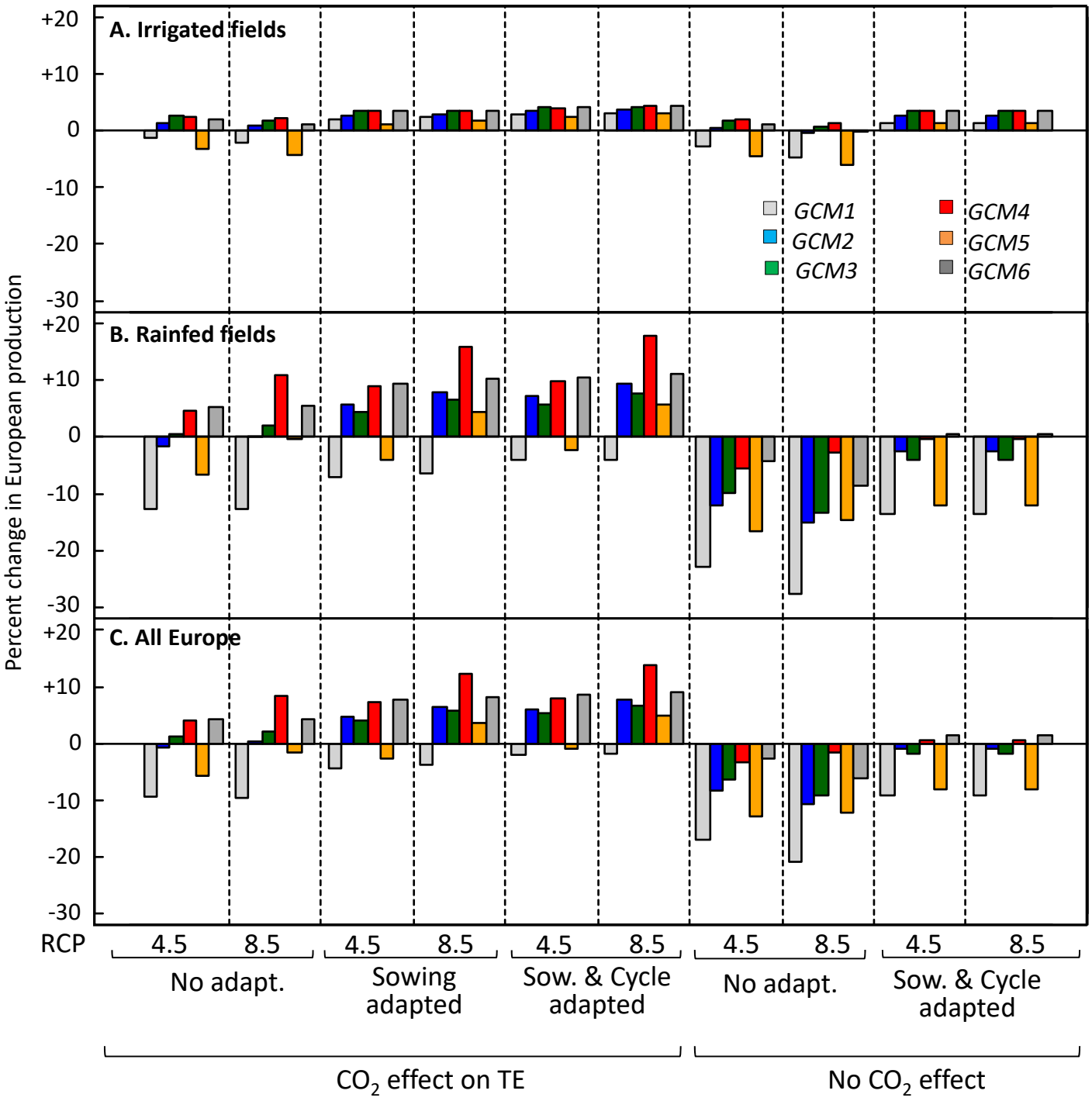

Supplementary Figure 11. Impact of climate change on European maize production depending on farmer adaptation to climate change in scenarios RCP4.5 and RCP8.5 for 6 GCMs, under two hypothesis for the CO_2 effect on transpiration efficiency (TE). Impacts were calculated by considering that the maize growing area and access to water will be the same in 2050 compared to the baseline period (1975-2010). The proportion in whole Europe was calculated by taking into account the proportion of irrigated vs rainfed area for maize in each grid cell of the Eurostat database. Colors display results for each of the six tested GCMs. GCM1: GFDL-CM3 , GCM2 HadGEM2-ES , GCM3: MIROC5 , GCM4: MPI-ESM-MR , GCM5: CMCC-CM , GCM5: MIROC-ESM.

A	Sowing date current	Sowing date 2050 (RCP4.5)	Sowing date 2050 (RCP8.5)	Change (day) baseline-RCP4.5	Change (day) baseline-RCP8.5
Mean	10th April	21th March	19th March	-20	-22
Median	10th April	25th March	20th March	-19	-22
min	20th March	17th Febr.	7th Febr.	-39	-41
max	30th April	20th April	17th April	-10	-9

B

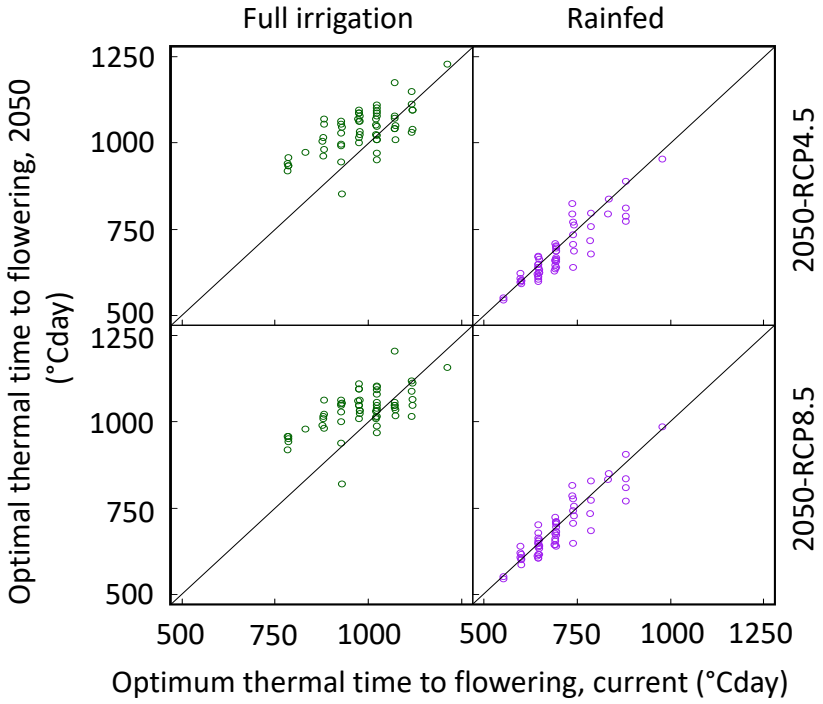

Supplementary Figure 12. Optimal sowing date and relationship between current and future optimal time to flowering. A, Table of optimal sowing date in the baseline period (1975-2010) and for two RCPs in 2050. **B,** Relationship between optimal time to flowering in the baseline period and for RCP4.5 and RCP8.5 in the 59 European sites under irrigated or rainfed conditions. Lines are the 1:1 relationships.

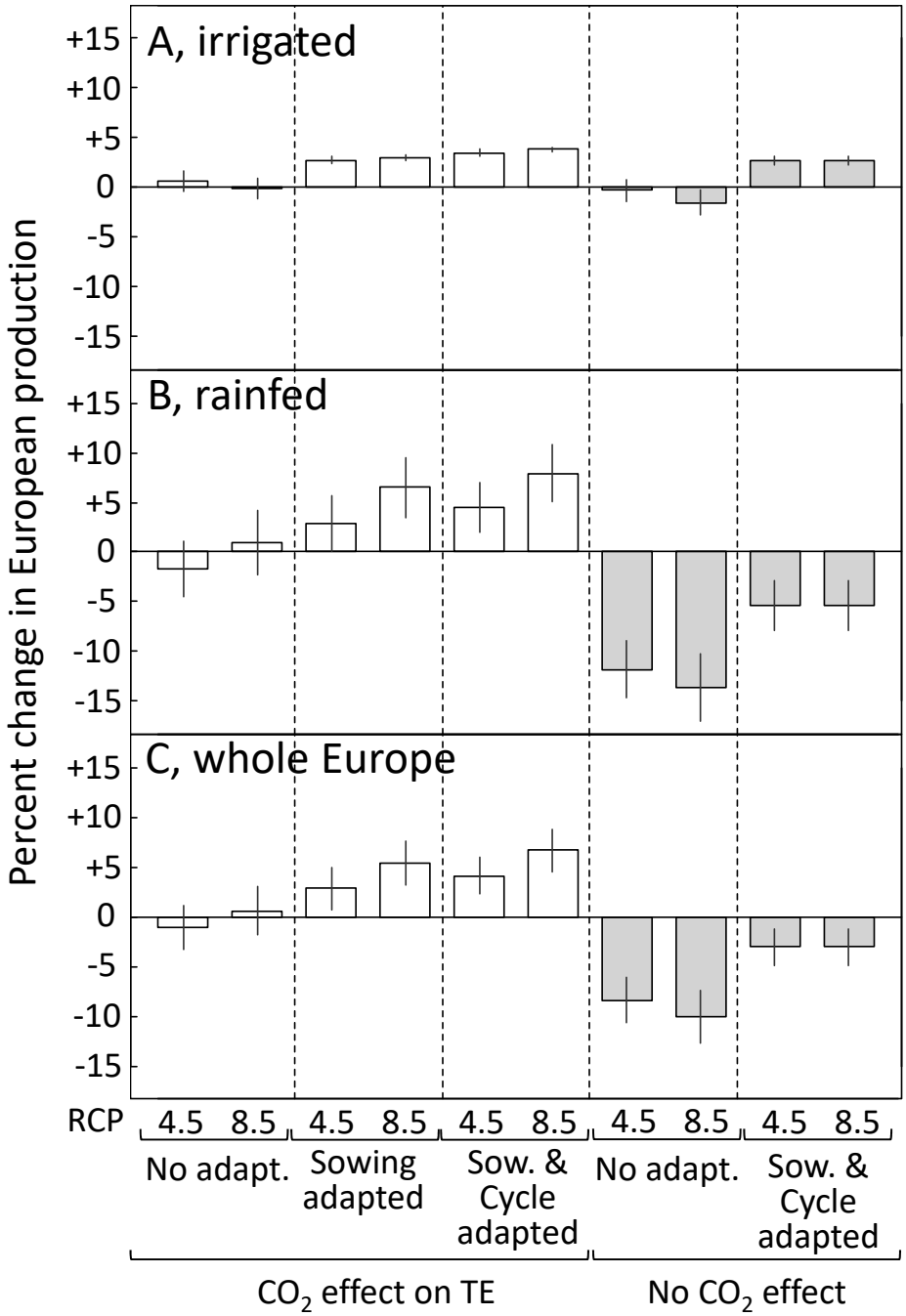

Supplementary Figure 13. Impact of climate change on European maize production depending on farmer adaptation to climate change in scenarios RCP4.5 and RCP8.5, under two hypothesis for the CO_2 effect on transpiration efficiency (TE), in well-watered conditions (A), rainfed conditions (B) or whole Europe (C). The latter calculation considered the proportion of irrigated vs rainfed maize fields in the Eurostat 25x25 km grid cells. Simulations consider that the maize area and access to water will be the same in 2050 compared with the 1975-2010 period, and the hypothesis of an increase in transpiration efficiency (TE) with CO_2 concentration. White, no adaptation; grey, adaptation of sowing date and cycle duration. Simulations for individual GCMs, with or without change in TE, are in Fig. SI 11. Error bars, standard error calculated over the six considered GCMs.

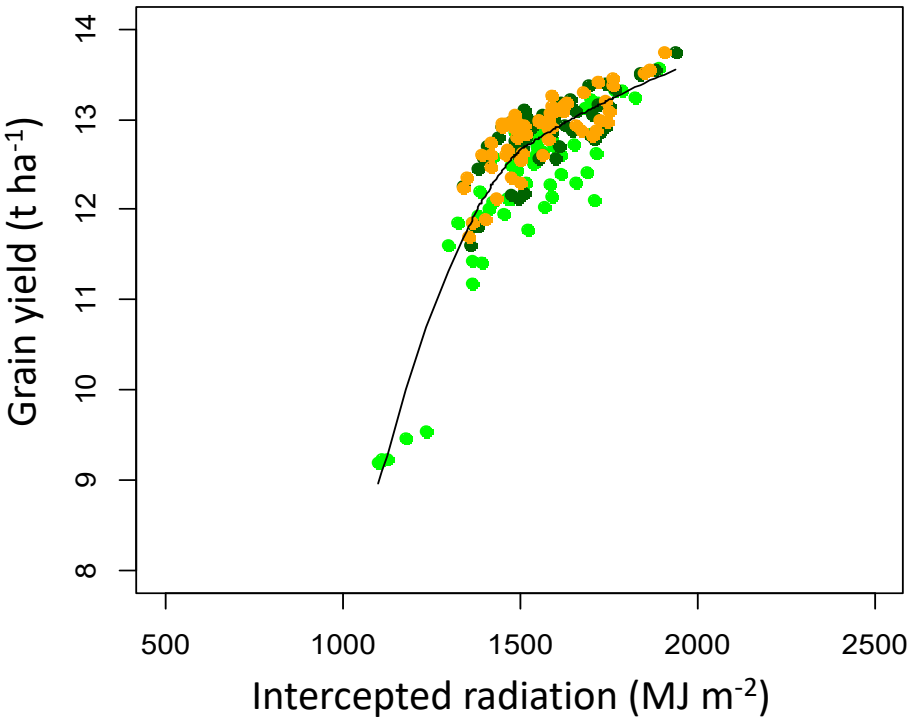

Supplementary Figure 14. Relationship between simulated intercepted light and simulated grain yield in irrigated conditions for the baseline period (1975-2010) and for two RCPs in 2050. Each dot is the average value for one site for the baseline period (green) or in 2050 for RCP4.5 (dark green) or RCP8.5 (orange).

Supplementary Table 1. Summary of maize growing sites used in simulations, proportion of irrigated in each site and ratio of maize harvested area per country.

Site	Longitude (°)	Latitude (°)	Irrigation
Austria_Leibnitz	15.6	46.8	0.01
Bulgaria_General_Toshevo	28.0	43.7	0.01
Bulgaria_Glavinitsa	26.8	43.9	0.00
France_Achenheim	7.6	48.6	0.34
France_Avignon	4.8	43.9	0.80
France_Chemille	-0.7	47.2	0.23
France_Clermont_Ferrand	3.1	45.8	0.36
France_Estrees_Mons	3.0	49.9	0.02
France_Marmande	0.2	44.5	0.48
France_Montelier	5.0	45.0	0.33
France_Orthez	-0.8	43.5	0.48
France_Ouges	5.1	47.3	0.09
France_Palaminy	1.1	43.2	0.68
France_Pamproux	-0.1	46.4	0.44
France_Patay	1.7	48.1	0.56
France_Saint_Bonnet	0.1	45.5	0.44
France_Toulouse	1.4	43.6	0.68
France_Vitre	-1.2	48.1	0.23
Germany_Augsburg	10.9	48.4	0.00
Germany_Hanover	9.7	52.4	0.49
Germany_Werl	7.9	51.6	0.00
Greece_Evropos	22.6	40.9	0.85
Hungary_Foldeak	20.5	46.3	0.06
Hungary_Kondoros	20.8	46.8	0.06
Hungary_Kormend	16.6	47.0	0.13
Hungary_Lajoskomarom	18.3	46.9	0.01
Hungary_Nyirbator	22.1	47.8	0.08
Hungary_Ormenyes	20.6	47.2	0.08
Hungary_Papa	17.5	47.3	0.01
Hungary_Szederkeny	18.5	46.0	0.00
Italy_Asola	10.4	45.2	0.60
Italy_Bologna	11.4	44.5	0.00
Italy_Campoformido	13.2	46.0	0.00
Italy_Orgiano	11.5	45.4	0.00
Italy_Paese	12.2	45.7	0.00
Italy_Pantigliate	9.4	45.4	0.60
Italy_Santena	7.8	45.0	0.60
Poland_Tuszyn	16.7	50.8	0.00
Poland_Wrzesnia	17.6	52.3	0.00
Romania_Alexandria	25.4	44.0	0.01
Romania_Arad	21.3	46.2	0.06
Romania_Barca	23.6	44.0	0.03
Romania_Barlad	27.7	46.2	0.00
Romania_Botosani	26.7	47.8	0.00
Romania_Bulbacata	25.8	44.3	0.01
Romania_Chirnogeni	28.2	43.9	0.01
Romania_Daia_Romana	23.7	46.0	0.00
Romania_Dochia	26.6	46.9	0.00
Romania_Dor_Marunt	26.9	44.4	0.01
Romania_Gataia	21.4	45.4	0.00
Romania_Lovrin	20.8	46.0	0.00
Romania_Medgidia	28.3	44.3	0.05
Romania_Parscoveni	24.2	44.3	0.01
Romania_Puchenii_Mari	26.1	44.8	0.01
Romania_Salard	22.0	47.2	0.08
Romania_Viziru	27.7	45.0	0.05
Spain_Barbues	-0.4	42.0	0.93
Spain_Gomecello	-5.5	41.1	0.80
Spain_Villamanan	-5.6	42.3	0.80

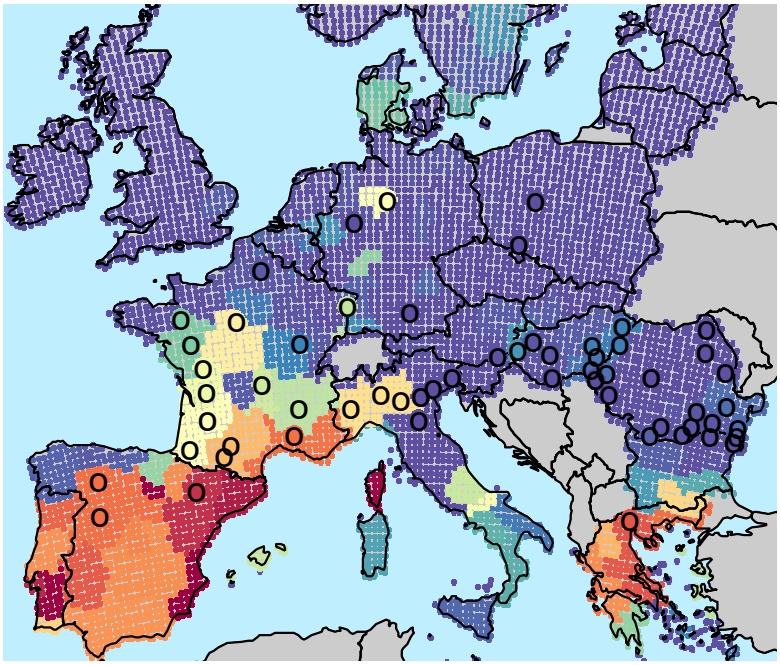

Proportion of irrigated maize fields

0 0.25 0.5 0.75 1

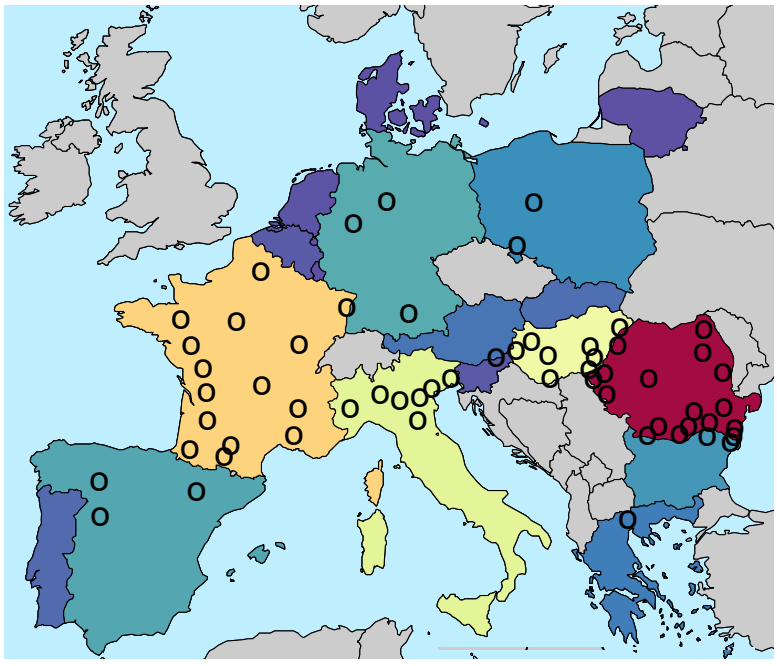

Proportion of maize growing area in each country compared to total European maize area

0 0.1 0.2 0.3